The Proposal of Simplified Truss Model for Shear Carrying Capacity of Prestressed Concrete Beams

M. Lertsamattiyakul[1)], J. Niwa[2)], S. Tamura[3)], and Y. Hamada[3)]

1) Doctoral Student, Department of Civil Engineering, Tokyo Institute of Technology, Japan
2) Professor, Department of Civil Engineering, Tokyo Institute of Technology, Japan
3) Researcher, Research and Development Center, DPS Bridge Work Co., Ltd, Japan
96b31110@cv.titech.ac.jp, jniwa@cv.titech.ac.jp, s_tamura@dps.co.jp, y_hamada@dps.co.jp

Abstract: In this study, the simplified truss model with a small number of members has been proposed for evaluating the shear carrying capacity and the failure pattern of PC slender beams without transverse reinforcement. To investigate the failure mechanism, which is influenced mainly by prestressing force and type of the stress distribution, the parametric study using FEM has been carried out. The estimated inclination of the critical stress flow and the thickness of struts assessed in terms of the width of bearing plates and the effective depth have been utilized to the proposed model. The satisfactory prediction on the shear carrying capacity and failure pattern of PC slender beams without transverse reinforcement can be obtained.

1. INTRODUCTION

With the requirements of saving in dead load resulting from the concrete section together with a high resistance in the superhigh-rise structures, prestressed concrete (PC) becomes the significant structural members. At present, it is recognized that the clear explanation and the well-predicted analytical results for the shear failure behavior of PC beams are still not achieved. For the recommended method by JSCE (2002) called the decompression moment method, the scatter of predicted results is usually observed due to the neglecting of distribution of the prestressing force. Moreover, there is another method considering the resistance at the flexural cracking as the extra value to the shear resistance due to the contribution of compression, called M_{cr} method (Ito et al. 1994). It has been observed that, even in PC slender beams where shear span to effective depth ration, a/d, ≥ 2.5, after the diagonal cracking, the beams still maintain the resistance due to the arch action and finally fail in shear compression mode. It is found that this method cannot be used to yield the comprehensive explanation about the shear compression failure of PC slender beams and how the resistance of the flexural cracking remains until the ultimate stage. Thus, newly proposed method should be simple, accurate in prediction and able to clarify the mechanism of shear compression failure by considering the effects of prestressing forces and type of stress distribution.

In this study, the simplified truss model has been proposed to assess the shear carrying capacity of PC slender beams without transverse reinforcement. To obtain the important information for modeling, the parametric study using finite element method (FEM) of PC slender beams has been performed. The failure mechanism influenced by the variation of significant parameters has been clarified. The tendency of stress flows obtained from the analytical results is summarized and adopted to the model. The shear carrying capacity and the failure patterns of the calculated and experimental results are compared in order to confirm the applicability of the proposed model.

2. PARAMETRIC STUDY USING FEM

To investigate the failure mechanism of PC slender beams, the nonlinear FEM analysis using DIANA system has been carried out. Details of geometric properties of the analytical model are illustrated in Figure 1. The values of prestressing force, P, in the upper and lower prestressing bars are proportionally adjusted and varied in the range of 100- 400 kN. Based on the values of P and the location of applied axial force, the upper and lower fiber stresses (σ_u and σ_l, respectively) are calculated and changed in the range of –3- 6 and 1- 15 MPa, respectively. From the values of σ_u and σ_l, the types of stress distribution can be categorized into 4 types as shown in Figure 2. The shear span to effective depth ratio, a/d, the effective depth, d, and the compressive strength of concrete, f_c', are also considered as the significant parameters and varied from 2.5- 4.5, 400- 800 mm and 40- 80 MPa, respectively. The width of beam, b, is assumed to be 200 mm for all cases. The longitudinal reinforcement ratio is set to be 1.3% (f_{py} = 930 MPa).

The samples of contour figures of stress flow at 90% analytical resistance at the ultimate stage (90%V_{max}) of PC slender beams under triangle with zero upper fiber stress distribution (σ_u = 0 MPa) are depicted in Figure 3. It is found that, with the increase in σ_l, the slope of the concentrated stress flow becomes steeper (Figures 3(a) and (b)). However, when the value of σ_l becomes comparatively large, the concentration of this steep stress flow becomes weak, whereas the stress flow from the loading point to the support becomes remarkable (Figures 3(c) and (d)). It implies that, not only the resistance along the diagonal crack, the stress flow curvedly transferring to the support also exists. The comparison between the differences in types of stress distribution (variation of σ_u) is expressed as the example in Figure 4. With the increase in value of σ_u, the inclination of the stress flow becomes slightly steeper (Figures 4(a) and (b)). On the other hand, the stress flow curvedly transferring to support becomes larger with the greater value of σ_u (Figures 4(c) and (d)). That means, not only the value of σ_l, but the value of σ_u also influences on the inclination of concentrated stress flow. The estimation of inclination of the concentrated

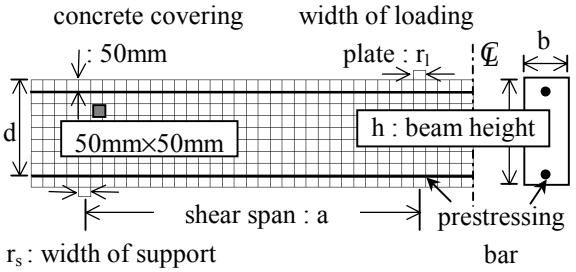

Figure 1 Finite element analytical model of PC slender beam in the parametric study

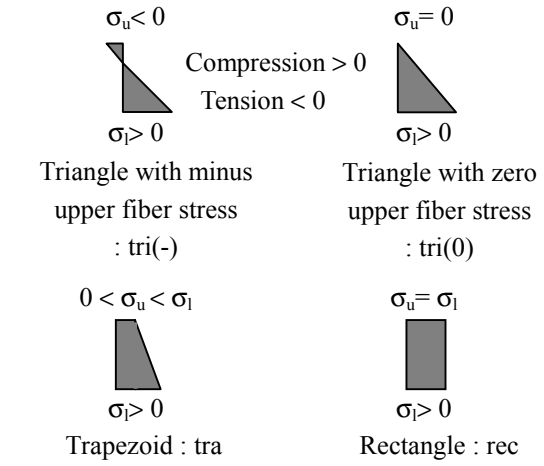

Figure 2 Types of stress distribution due to the prestressing force

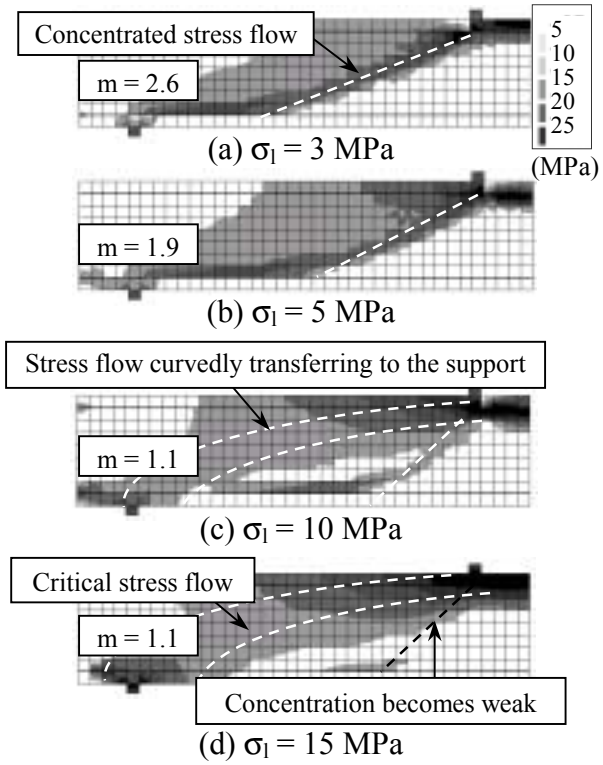

Figure 3 Analytical results with variation of σ_l where σ_u = 0 MPa
(a/d = 3.5, d = 400 mm and f_c'= 40MPa)

stress flow is important for predicting the failure mechanism of the beams. Therefore, the values of principal compressive stress, σ_2, at each Gauss's point are taken into the consideration. As demonstrated in Figure 5, between the upper and lower prestressing bars, the maximum absolute values of σ_2 in each horizontal level, $\sigma_{2i\text{-}max}$, are marked. By considering the location of $\sigma_{2i\text{-}max}$ as the co-ordination in X-Y axes, (x_i, y_i), the correlation coefficient (equation in Figure 5) is employed to express the level of correlation between the values of x and y in the approximated relationship. The part of marked Gauss's points that has a high value of correlation coefficient (≥ 0.95) is selected. The relationship of the selected points is approximated and summarized in terms of *m*, where $m = \cot\theta$ and θ is an angle of the estimated slope. It should be noted that the value of *m* decreases with the increase in the value of σ_l (Figure 3) and also slightly decreases with the increase in the value of σ_u (Figure 4). For the case that the stress flow curvedly transferring to support becomes the critical path, even though the concentration of the steep stress flow becomes weak, this steep inclination is assumed to evaluate the value of *m*. This is in order to recapitulate the values of *m* in the same trend that is the value of *m* decreases with the increase in the value of σ_l. The relationships between the values of *m* and σ_l with σ_u, *a/d*, *d*, and f_c' are summarized. As the example, in Figure 6**,** the relationship between the values of *m* from FEM results (FEM) and σ_l with σ_u are summarized and approximated (Approx.). It is found that the values of *m* become greater with the increase in values of *a/d* and f_c', while the value of *d* has a small effect on value of *m*. The equation for predicting the value of *m* can be expressed as in Eq. (1).

$$m = 2.55\left(\left(1+0.2\frac{\sigma_u}{\sigma_u+\sigma_l}\right)\sigma_l\right)^{-\frac{3}{5}}\left(\frac{a}{d}\right)\left(\frac{f_c'}{100}\right)^{\frac{3}{5}} \quad (1)$$

3. SIMPLIFIED TRUSS MODEL

Figure 7 demonstrates the simplified truss model with the prestressing forces in terms of the axial forces, P_1 and P_2, developed in this study to

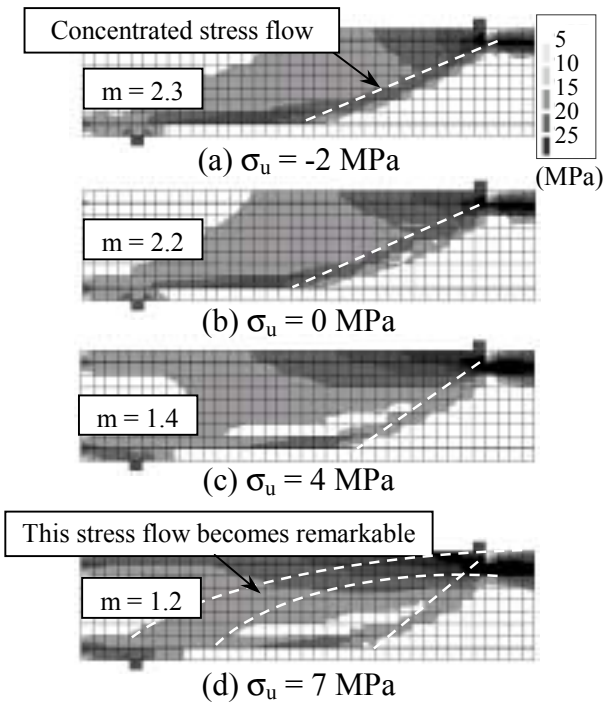

Figure 4 Analytical results with variation of σ_u where σ_l = 7 MPa
(a/d = 3.5, d = 400 mm and f_c'= 40MPa)

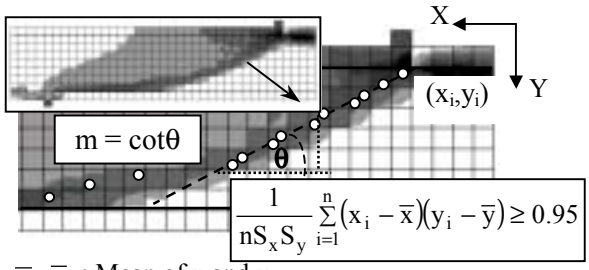

$\bar{x}$, $\bar{y}$: Mean of x and y
S_x, S_y : Standard division of x and y
n : Number of considered data

Figure 5 Evaluation of inclination of concentrated stress flow in terms of m

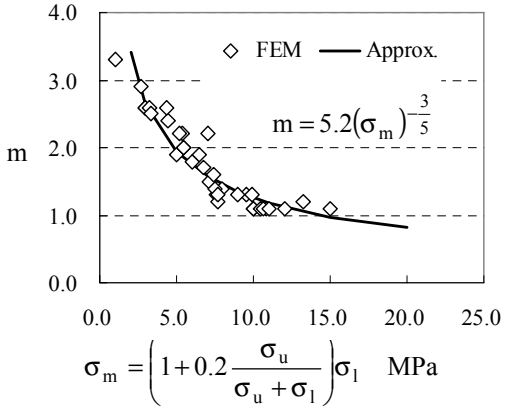

Figure 6 Relationship of m and σ_l and σ_u
(a/d=3.5, d=400mm, f_c'=40 MPa)

calculate the shear carrying capacity of PC slender beams without transverse reinforcement. As one of the main concepts that the model should be simple, the proposed model consists of 7 nodes and 11 members. The modeling of concrete and reinforcement are expressed as in Figure 7. After modeling by using the value of m, each member force, F_i, caused the externally applied shear force, V, can be determined by employing the principles of virtual work method. The equivalent elastic analysis has been carried out for simplicity in calculation. That is, the stiffness of concrete at the ultimate stage as the secant modulus and the concrete softening, η, are incorporated to the struts. The shear carrying capacity of the beam can easily be determined when the member force of one of 4 struts becomes greater than its capacity. The process of calculation is summarized in Figure 8. The location of two struts, [3] and [4], is simply assumed with the same horizontal distance in the level of flexural tension members as shown in the figure. The thickness of the flexural compression member is set to be $2c$, where c is the thickness of concrete cover. The thicknesses of the transverse tension members [5] and [6] are assumed to be the distance from the loading point to the middle point between members [5] and [6] and the left distance to the middle point of support, respectively. The sum of cross sectional area of reinforcements is applied as the cross sectional area of the flexural tension member. It is recognized that the thickness of strut is important for evaluating the resistance of concrete structure in shear compression failure.

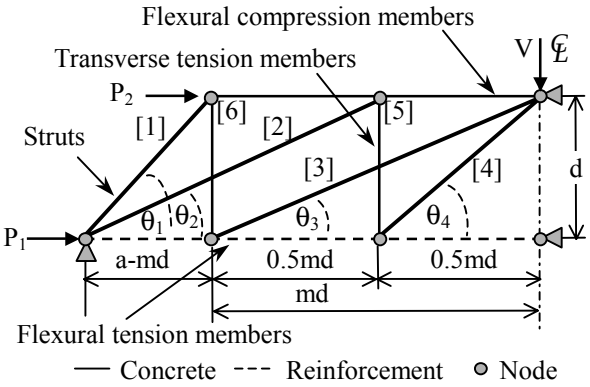

Figure 7 Simplified truss model for a PC beam without transverse reinforcement

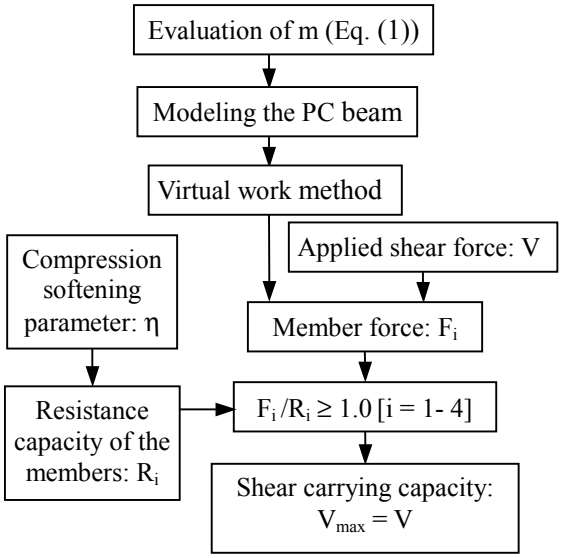

Figure 8 Process in calculating the shear carrying capacity

3.1 Thickness of Strut

Based on FEM analytical results, compressive stresses in the vertical direction at each Gauss's points, σ_{yi}, at about 90% of V_{max} are considered. The range of 0.2d inner side of a beam from the upper prestressing bar is investigated. In each level, the distribution of the ratio of σ_{yi} and the maximum values in that horizontal level, $\sigma_{yi\text{-}max}$, ($\Delta_i = \sigma_{yi}/\sigma_{yi\text{-}max}$) along the beam axis is evaluated. For each horizontal level of Gauss's point in the range of $0.2d$, the horizontal width of the distribution, t_i, where $\Delta_i = 0.3$ is measured. The average value of t_i is considered as the horizontal thickness of the strut, t. The range in the vicinity area of the support above the lower prestressing bar is also treated with the same process to evaluate the horizontal width of the distribution. Figure 9 shows the examples of obtained horizontal

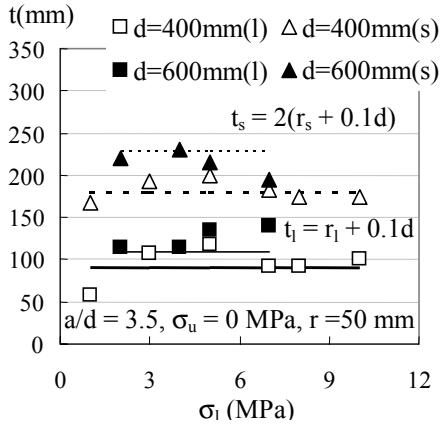

Figure 9 Example of measured and estimated t (variations of σ_l (σ_u = 0MPa) with d)

thickness in the vicinity area of a loading point, t_l, and support, t_s, from FEM analytical results with the variations of σ_l and d. By considering the effects of bearing plates and the effective depth (Niwa 1984), the values of t_l and t_s can be simply estimated with the width of a loading plate, r_l, or support, r_s, and d as r_l+0.1d and 2(r_s+0.1d), respectively. In the proposed model, the members [1] - [2], and members [3] - [4] are considered to be affected by support and loading plates, respectively. The cross sectional area of each strut can be assumed as the values of t_l or t_s multiplied with b and its inclination.

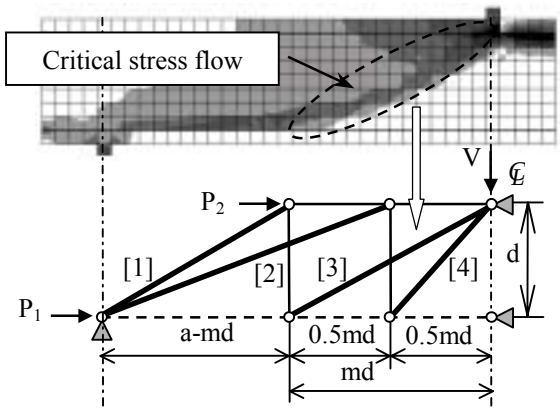

(a) Model 1: m > 1.0

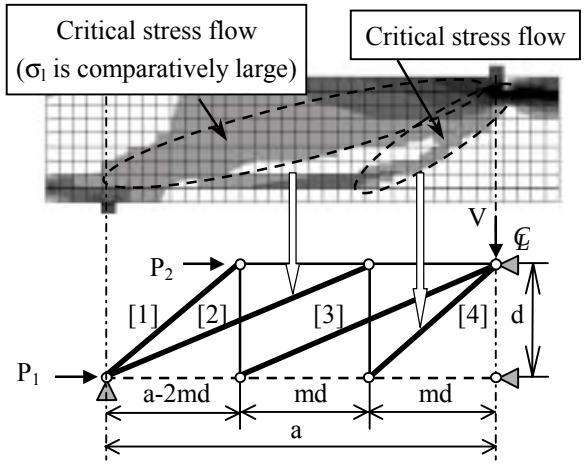

(b) Model 2: m ≤ 1.0

Figure 10 Division of the proposed simplified truss model

3.2 Division of Modeling

As discussed in the previous section, based upon the analytical study, there are 2 types of failure pattern can be observed. One takes place along the concentrated stress flow (Model 1) and the other one occurs along the stress flow curvedly transferring to the support (Model 2). By considering the value of m relating with the possible location of the critical strut, the proposed simplified truss model is divided into 2 models as depicted in Figure 10.

In *Model 1* (m > 1.0, Figure 10(a)), the distance md is adopted as the horizontal distance from the loading point to the ended node of member [3]. When $m \geq 2.0$, since the effect of a loading plate is considered to become weak, the thickness of member [3] is set to be $(a\text{-}md)\sin\theta_3$, where $d \geq a\text{-}md$. When the inclinations of struts are quite flat in case of $m \geq 2.0$, 50 mm is set to be a lower bound value of w_i avoiding the underestimation. The applied upper bound value of m is set to be $0.9a/d$ in modeling. The specimen with low up to medium level of prestressing stress is considered to match with this model.

In *Model 2* ($m \leq 1.0$, Figure 10(b)), the distance md is adopted as the horizontal distance from the loading point to the ended node of member [4]. Due to the small effect of bearing plates on the size of members [2] and [3], which are expressing the stress flow curvedly transferring to the support, the thicknesses are set to be $md\sin\theta_2$ and $(a\text{-}2md)\sin\theta_3$, where $d \geq a\text{-}2md$. Because of the inclinations of struts are quite flat, 50 mm is assumed as a lower bound value of w_i in this case. This model is considered to fit for a specimen with comparatively high prestressing stress level.

3.3 Compression Softening Parameter

In calculation of the shear carrying capacity, the value of compression softening parameter, η, affected by the existence of cracks, should be considered. For a sake of simplicity in calculation, the practical expression of η is equated with a slight variation from 0.6 to 0.4 in the range of f_c' of 30 to 100 MPa as in Eq. (2).

$$\eta = -0.3\left(\frac{f_c'}{100}\right) + 0.7 \tag{2}$$

4. COMPARISON OF CALCULATED AND EXPERIMENTAL RESULTS

The outlines of the specimens and comparisons between the experimental and calculated results in order to confirm the applicability of the simplified truss model are tabulated in Table 1. By checking the reliability of the test data by FEM as in the previous study (Tamura et al 2003) and the additional investigation, 31 cases of the experimental results from 9 references are collected (Arai et al 2000, Hamada et al 1999, Kar 1969, Kobayashi 1992, Mikata et al 2001, Mikata 2002, PWRI 1995, Sato et al 1987, Tamura et al 2001). All specimens failed by the shear compression mode of failure. The data consist of the wide ranges of geometric properties, that is, the values of *a/d* vary in the range of 2.4 to 5.1 and the values of *d* change from 140 to 1000 mm. The prestressing force in terms lower fiber stress vary from 2.0 to 21.0 MPa including all 4 types of stress distribution. In case that the roller loading was applied, the value of width of the bearing plate is set to be 50 mm in calculation. In Table 1, the number of critical strut mentioned in Figure 10 is written for each case. It is evident that the calculated results yield the well-predicted results compared with the experimental results, in many conditions of concrete properties, geometric properties, level of

Table 1 Outline of experimental data and the comparison with the calculated results

Researcher	No.#	Specimen	a/d	d (mm)	f_c' (MPa)	r_l/r_s* (mm)	σ_u (MPa)	σ_l (MPa)	m	m** (model)	$V_{exp.}$ (kN)	η	$V_{cal.}$ (kN)	$V_{exp.}/V_{cal.}$	Failed member
Arai	1	*NC-40*	3.0	167	36.4	50/50	-0.1	4.3	1.7	1.7	41	0.59	38	1.08	3
	2	*NC-80*	3.0	167	36.4	50/50	-0.2	8.3	1.2	1.2	46	0.59	42	1.10	2
	3	*LC-40*	3.0	167	36.5	50/50	-0.1	4.3	1.7	1.7	35	0.59	38	0.92	3
	4	*LC-80*	3.0	167	36.5	50/50	-0.2	8.3	1.2	1.2	36	0.59	42	0.86	2
	5	*SC-40*	3.0	167	37.4	50/50	-0.1	4.3	1.8	1.8	27	0.59	37	0.73	3
	6	*SC-80*	3.0	167	37.4	50/50	-0.2	8.3	1.2	1.2	33	0.59	43	0.77	2
Hamada	7	45LC-0	3.5	300	47.0	65/150	-1.2	3.4	2.9	2.9	135	0.56	123	1.10	4
Kar	8	A-1	5.1	175	35.9	100/100	-1.0	6.0	2.5	2.5	26	0.59	23.0	1.13	2
	9	A-2	5.1	175	34.8	100/100	0.0	5.0	2.6	2.6	24	0.60	23.0	1.04	2
Kobayashi	10	*L5*	2.4	167	38.0	R/R	0.0	3.9	1.5	1.5	63	0.59	58	1.09	3
Mikata	11	P-0-20	3.2	140	41.9	R/R	0.0	2.0	3.2	2.9	49	0.57	50	0.98	2
	12	P-0-30	3.2	140	43.0	R/R	0.0	3.0	2.6	2.6	53	0.57	47	1.13	2
	13	P-0-40	3.2	140	43.0	R/R	0.0	4.0	2.1	2.1	48	0.57	49	0.98	2
	14	P-20-40	3.2	140	43.0	R/R	2.0	4.0	2.1	2.1	52	0.57	49	1.06	2
	15	P-40-40	3.2	140	43.0	R/R	4.0	4.0	2.0	2.0	48	0.57	50	0.96	2
	16	HP-0-30	3.2	140	79.6	R/R	0.0	3.0	3.7	2.9	74	0.46	72	1.03	2
Mikata	17	*PRC-9*	2.6	152	60.0	R/R	-1.0	12.2	1.1	1.1	63	0.52	83	0.76	2
	18	*PRC-12*	2.6	152	72.1	R/R	-1.7	21.1	0.9	0.9	100	0.48	105	0.95	3
PWRI	19	H3-35-30	3.0	350	92.0	100/150	-1.0	3.0	4.0	2.7	245	0.42	251	0.98	4
	20	H3-35-60	3.0	350	86.3	100/150	-2.0	6.0	2.5	2.5	284	0.44	311	0.91	4
	21	H3-35-90	3.0	350	70.3	100/150	-3.0	9.0	1.8	1.8	295	0.49	257	1.15	3
	22	H3-55-30	3.0	550	84.0	100/150	-1.0	3.0	3.8	2.7	228	0.45	282	0.81	4
	23	H3-75-30	3.0	750	88.5	100/150	-1.0	3.0	3.9	2.7	345	0.43	316	1.09	4
	24	H3-95-60	3.0	950	71.4	100/150	-2.0	6.0	2.3	2.3	586	0.49	583	1.01	3
	25	L3-35-60	3.0	350	40.6	100/150	-2.0	6.0	1.6	1.6	202	0.58	190	1.06	3
Sato	26	*3-11*	2.5	403	41.8	R/150	-3.1	8.9	1.1	1.1	171	0.57	193	0.89	3
	27	*4-6*	3.2	337	40.1	50/50	-5.0	14.0	1.0	1.0	170	0.58	185	0.92	3
	28	*4-12*	3.1	353	39.7	50/50	-4.7	14.5	1.0	1.0	162	0.58	190	0.85	3
Tamura	29	45LC-3	3.8	1000	55.1	150/150	-1.1	2.6	4.1	3.4	505	0.53	406	1.24	3
	30	45LC-5	3.8	1000	53.3	150/150	-2.0	5.0	2.7	2.7	569	0.54	684	0.83	2
	31	60LC-5	3.8	1000	68.7	150/150	-2.4	5.8	2.9	2.9	600	0.49	734	0.82	2
													AVE.	0.97	
													C.V.	0.13	

 # : Model 2 is in bold.

** : Unit is MPa Italic characters : Prestressed reinforced concrete beams*

*** : Applied values of m in modeling : Lightweight concrete*

prestressing force and the types of stress distribution. The comparisons between the crack patterns at the ultimate stage and the failed members of the predicted results are also carried out. As the examples shown in Figure 11, the good agreement between the critical strut and the crack patterns of specimens, which are predicted to fail by the members [2], [3] and [4], can be observed. The bold dashed line represents the critical strut in each specimen. From the satisfactory prediction in case of the specimen P-40-40 as shown in Figure 11(a), it implies that this proposed simplified truss model is applicable for predicting the crack pattern even in case where σ_u is under compression (rectangular stress distribution). From Figures 11(b) and (c), it is apparent that this proposed model can be utilized to predict the failure patterns of the normal (H3-35-30) and lightweight (L5) PC slender beams. Moreover, it can also be said that the crack pattern of prestressed reinforced concrete beam can satisfactorily be estimated as shown in case L5 (Figure 11(b)).

In order to confirm the high accuracy in prediction, the calculated results of the proposed simplified truss model (*Proposed*) are compared with the calculated results of M_{cr} method (M_{cr}) (Ito et al 1994). The comparison is expressed in Figure 12 with the variation of lower fiber stress. It is found that the proposed model provides calculated results with the average value (AVE.) of 0.97 and a coefficient of variation (C.V.) of 0.13, whereas M_{cr} method yields the calculated results which AVE. = 1.18 and C.V. = 0.22. Based on these results, it can be said that the proposed model yields the better accuracy in prediction of shear carrying capacity.

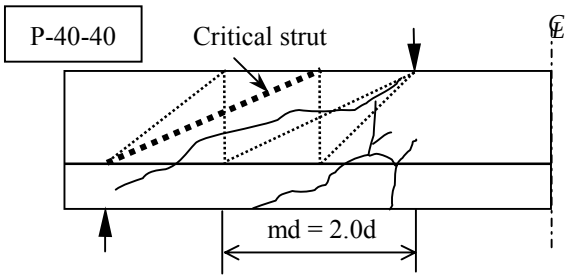

(a) Critical strut: Member [2]

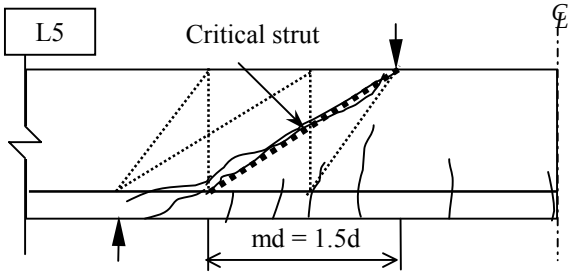

(b) Critical member: Member [3]

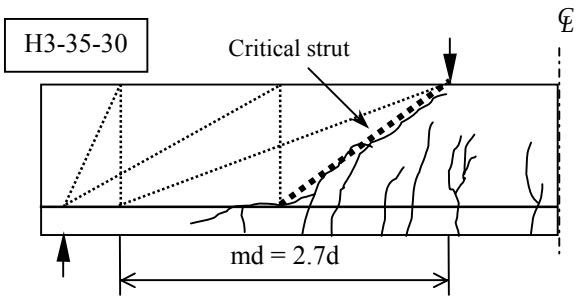

(c) Critical strut: Member [4]

Figure 11 Examples of the critical members and actual crack patterns at the ultimate stage

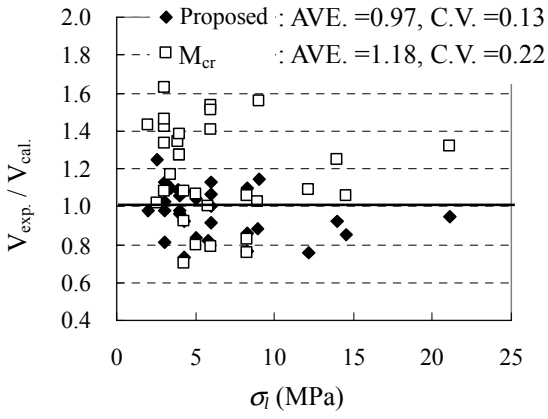

Figure 12 Comparison in shear carrying capacity between the proposed model and M_{cr} method

5. CONCLUSIONS

The simplified truss model has been proposed based on the clarification of failure mechanism in the parametric study using FEM. With the increase in value of σ_l, the inclination of critical stress flow becomes steeper. In case of considerably high value of σ_l, the concentrated stress flow turns into the stress flow curvedly transferring to the support. It can be said that the influence on the shear failure mechanism due to σ_u

(types of stress distribution) cannot also be neglected. For calculating the shear carrying capacity of PC slender beams, the equivalent elastic analysis of the simplified truss model with a small degree of freedom has been performed. The thickness of the considered struts assessing from FEM results is simply estimated in terms of the width of bearing plates and the effective depth. By adopting the evaluated thickness of struts and the value of *m*, the excellent correlation with the experimental data can be achieved. It is apparent that the simplified truss model is applicable to evaluate the shear carrying capacity and the failure patterns of PC slender beams without transverse reinforcement.

References:

Japan Society of Civil Engineers (JSCE) (2002), "Standard Specification for Concrete Structures," *Structural Performance Verification*.

Ito, T., Yamaguchi, T. and Ikeda, S. (1994), "Flexural Shear Behavior of Precast Segmental PC Beam," *Proceedings of the JCI*, **16**(2), 967-972.

Niwa, J. (1984), "Equation for Shear Strength of Reinforced Concrete Deep Beams Based on FEM Analysis," *Concrete Library of JSCE*, **4**, 283-295.

Tamura, S., Hamada, Y., Lertsamattiyakul, M. and Niwa, J. (2003), "A Study on Shear Carrying Capacity of Evaluation Methods of Prestressed Concrete Beams with Rectangular Cross Section," *Journal of Prestressed Concrete*, **45**(6), 101-110.

Arai, Y. and Yaginuma, Y. (2000), "Shear Behavior of PC Beams Using Light-weight Concrete," *Proceedings of The 10th Symposium on Developments in Prestressed Concrete*, 545-550.

Hamada, Y., Tamura, S., Maehori, S. and Niwa, J. (1999), "Ultimate Shear Capacity of Prestressed Concrete Beams Using High Performance Lightweight Aggregates," *Proceedings of The 9th Symposium on Developments in Prestressed Concrete*, 739-744.

Kar, J. N. (1969), "Shear Strength of Prestressed Concrete Beams Without Web Reinforcement," *Magazine of Concrete Research*, **21**(68), 159-170.

Kobayashi, K. (1992), "Effects of Introducing Prestress on Shear Resistance of Concrete Beams," *Proceedings of Cement and Concrete*, *Japan Cement Association*, **46**, 750-755.

Mikata, Y., Inoue, S., Kobayashi, K. and Nieda, T. (2001), "Effect of Prestress on Shear Capacity of Prestressed Concrete Beams," *Journal of Materials, Concrete Structures and Pavements, JSCE*, **669**(50), 149-159.

Mikata, Y. (2002), "The Study on Shear Strength Characteristics of Concrete Structural Members," *Doctoral Thesis*, Dept. of Civil Eng., Osaka Institute of Technology.

Public Works Research Institute (1995), "Study on Shear Strength of PC Beams with High Strength Concrete," *Joint Research on Design Method of High Strength Concrete Structures*, **122**.

Sato, T., Ishibashi, T., Yamashita, H. and Takada, S. (1987), "Shear Strength and Modes of Failure of Prestressed Concrete Beams," *Proceedings of the JCI*, **9**(2), 323-328.

Tamura, S., Hamada, Y., Maehori, S. and Niwa, J. (2001), "Shear Strength Characteristics of Large Scale PC Beams Using Super Lightweight Concrete," *Proceedings of the JCI*, **23**(3), 709-714.